ACTA CHEMICA SCANDINAVICA 16 (1962) 1–19

X-Ray Investigations of the Ternary System Fe-P-B. Some Features of the Systems Cr-P-B, Mn-P-B, Co-P-B and Ni-P-B

STIG RUNDQVIST

Institute of Chemistry, University of Uppsala, Uppsala, Sweden

The solid region of the Fe–P–B system has been investigated in the range Fe–FeP_2–BP–FeB–Fe by means of X-ray and chemical analyses. The main features of an isothermal section at 1 000°C have been determined. Boron substitutes for phosphorus to a large extent in Fe_3P and to a smaller extent in Fe_2P and FeP. Two ternary phases exist, *viz.* Fe_5PB_2, homogeneous in a relatively narrow composition range, and $Fe_3P_{1-x}B_x$ (denoted ε_1), homogeneous in the approximate range $0.48 < x < 1$ at 1 000°C.

Solid solubility of boron is appreciable in Cr_3P and Mn_3P, but is very restricted in Ni_3P. The ternary phase Mn_5PB_2 is isostructural with Fe_5PB_2. In the Co–P–B system, three ternary phases have been found, *viz.* $Co_3P_{1-x}B_x$, homogeneous in a narrow range near $x = 0.7$ and isostructural with the ε_1 phase in the Fe–P–B system, $Co_3P_{1-y}B_y$, homogeneous in a narrow range near $y = 0.5$ and isostructural with Fe_3P, and finally Co_5PB_2, isostructural with Fe_5PB_2 and Mn_5PB_2.

The crystal structures of Fe_3P, ε_1 (with the composition $Fe_3P_{0.37}B_{0.63}$), and Fe_5PB_2 have been determined and refined using single-crystal methods. The space-group of the ε_1 structure is $P\,4_2/n$ with 24 iron atoms in three sets of eightfold positions. The boron and phosphorus atoms are randomly distributed in one eightfold position. The structure is very closely related to that of Fe_3P. Fe_5PB_2 has the Cr_5B_3 ($D\,8_l$)-type structure. The distribution of the boron and phosphorus atoms is essentially ordered.

During investigations of borides, silicides and phosphides of the Group VII and VIII transition metals made at this Institute, some attention has been devoted to ternary systems containing one transition metal and two non-metals [1,2]. The present paper deals with X-ray investigations of the ternary system Fe–P–B and the closely related systems Cr–P–B, Mn–P–B, Co–P–B and Ni–P–B. As far as the author is aware, no earlier investigations of these systems have been published. The results will be presented in two main parts, the first dealing with the phase analyses and the second with the crystal structure determinations.

I. PHASE-ANALYTICAL INVESTIGATIONS

The preparation of pure Fe—P—B alloys in equilibrium proved difficult. Heat treatments must be made in closed containers to avoid phosphorus losses at high temperatures. Since the alloys sometimes react with silica, the simple method of heating the elements together in evacuated and sealed silica tubes leads to contamination, mostly by oxygen and also to some extent by silicon. Nevertheless, preliminary investigations of the Fe—P—B system were made on a large number of alloys of purities about 97 %, prepared by heating iron powder (98 %), red phosphorus (99 %) and boron (97 %) in silica tubes. The data obtained from these alloys were quite consistent and provided a rough general picture of the system. In order to substantiate the results, efforts were made to prepare a smaller number of pure alloys in selected parts of the system.

Experimental

Preparation

The starting materials were iron powder or iron rods (both *ex* Johnson, Matthey & Co. Ltd., London, spectrographically standardized, the former containing about 5 % oxygen, the latter only very small amounts of gaseous impurities), red phosphorus (purity higher than 99 %) and boron, (Borax Consolidated Ltd., London, purity higher than 99 %).

Master alloys of iron borides were made by sintering iron powder and boron in a high-frequency vacuum furnace as follows. The mixed powders were pressed into pellets and heated in crucibles of pure aluminium oxide (Degussit Al 23 from Degussa, Frankfurt) lined with boron nitride (Norton Company, Massachusetts). The boron oxide formed by reduction was separated magnetically, and the process of sintering and magnetic separation was repeated until no more boron oxide could be eliminated. The final products had a purity higher than 99.7 %, the remaining impurities being mainly oxygen.

Master alloys of iron phosphides were made by dropping pellets of red phosphorus into molten iron, contained in a Degussit Al 23 crucible. The melting was done by induction heating in a closed chamber filled with argon, previously purified over hot calcium chips and over hot turnings of a 1:1 titanium-zirconium alloy. On analysis, phosphides prepared in this way gave totals for iron and phosphorus between 99.94 % and 100.02 %.

Ternary Fe—P—B alloys were prepared as follows. Appropriate mixtures of the master alloys were melted rapidly in an argon-filled arc furnace using the lowest possible temperature to avoid excessive phosphorus losses. Equilibrium was attained only after prolonged heat treatment. For this purpose the alloys, contained in small alumina crucibles, were sealed under vacuum in silica tubes. The annealing time (after which no further changes were noticed on the powder photographs of the alloys) was generally 1—2 weeks, and the alloys were quenched in oil or water. Small amounts of oxygen unavoidably entered the alloys during the final heat-treatments, but the total amount of impurities in the final products could generally be kept below 1 %.

The ternary alloys containing chromium, manganese, cobalt or nickel were prepared by heating the elements directly in silica tubes. No chemical analyses were made, but from the appearance of the silica tube walls it was estimated that the impurity content of these alloys is no higher than that of the iron alloys made in the same way.

Chemical analysis

The chemical analyses were performed by the Analytical Department of this Institute.

Determination of iron and phosphorus. The sample was dissolved in *aqua regia* and iron and phosphorus were determined in separate aliquots of this solution.

For the determination of iron, the solution was evaporated with nitric acid, which was afterwards removed by evaporation with sulphuric acid. The diluted solution was passed through a cadmium reductor, and then titrated with 0.1 N cerium sulphate, previously standardized against a solution prepared from spectrographically pure iron rods (Johnson, Matthey & Co, London).

Phosphorus was determined as follows. The solution was evaporated twice with nitric acid to remove the hydrochloric acid, and the residue dissolved in perchloric acid. Oxidation to orthophosphoric acid was completed by boiling the solution for a few minutes. Phosphorus was determined by precipitating ammonium molybdophosphate and weighing as $P_2O_5 \cdot 24MoO_3$ according to Nydahl [3].

Determination of boron. The sample was dissolved by refluxing with dilute sulphuric acid, hydrogen peroxide and a few drops of hydrochloric acid. The boric acid was separated as methyl borate by distillation, and titrated potentiometrically with sodium hydroxide in the presence of mannitol.

X-Ray methods

X-Ray powder photographs were taken with Guinier-type focussing cameras using Cr*Ka* radiation and with calcium fluoride (a = 5.4630 Å) or silicon (a = 5.4305 Å) as internal calibration standards. Although the accuracy of a single lattice parameter determination is not claimed to be higher than 0.04 %, lattice parameter differences larger than 0.02 % for a given phase, measured in different alloys, are considered significant.

The binary boundary systems

Fe—P. The system has been investigated by several methods, and previous work is summarized in Ref.[4]. The existence of the intermediate phases Fe_3P, Fe_2P, FeP and FeP_2 has been demonstrated. The existence of phosphides with a phosphorus content higher than FeP_2 has also been claimed [5].

Fe—B. The system has been investigated in the range 0—50 atom % boron (for references, see Ref.[4]). Two intermediate phases exist, *viz.* Fe_2B and FeB. It has been claimed that FeB has two modifications [6]. In the present work only the normal *B* 27 structure for FeB was observed.

B—P. This system is still incompletely known. The existence of the compound BP, first reported by Besson [7] and Moissan [8,9], has been confirmed by several investigations [10–12]. The existence of B_5P_3, claimed by Moissan [9], has not been confirmed, but a boron phosphide of the approximate composition $B_{13}P_2$ has been prepared by Matkovich [13].

During the present investigation, the author observed the appearance of BP in ternary Fe—P—B alloys. BP was sometimes obtained as orange-red, octahedral crystals of remarkable hardness. Weissenberg photographs of these crystals confirmed the proposed zincblende structure. Heating boron and phosphorus in evacuated and sealed silica tubes yielded BP as the only identifiable reaction product. However, when BP was heated strongly in an argon-filled arc furnace, some phosphorus volatilized, leaving a very hard, grey-black residue. The powder photographs of this substance showed the presence of boron together with another phase, which gave diffraction data in close agreement with those quoted by Matkovich [13] for $B_{13}P_2$. No traces of $B_{13}P_2$ were, however, found in Fe—B—P alloys. This phase is presumably formed only at temperatures higher than 1 100°C.

Table 1. Crystallographic data for the binary phases. (Unit cell dimensions (Å) determined in the present investigation).

Compound	*Space group*	*Structure type*	*a*	*b*	*c*
Fe_3P	$I\,\bar{4}$	$D\,0_c$	9.107	—	4.460
Fe_2P	$P\,\bar{6}2m$	C 22 *	5.865	—	3.456
FeP	$Pnma$	B 31	5.191	3.099	5.792
FeP_2	$Pnnm$	C 18	4.971	5.654	2.719
Fe_3B	$I\,4/mcm$	C 16	5.109	—	4.249
FeB	$Pnma$	B 27	5.502	2.948	4.057
BP	$F\,\bar{4}3m$	B 3	4.538	—	—

* revised structure type [22].

The ternary system Fe—P—B

Since the author was primarily interested in the crystal structure data of the Fe—P—B system, only X-ray and chemical analyses were used in this investigation. Although in general, accurate determinations of phase-boundaries and tie-lines were not attempted, the main three-phase equilibria were determined. In addition, lattice parameters were determined for the binary phases (see Table 1) and for all phases appearing in the various three-phase triangles (see Table 2). The isothermal section of the Fe—P—B system given in Figs. 1 and 2 was constructed using results from the phase-analyses of alloys annealed at 1 000° for 7—14 days and quenched. The investigation was restricted to the range Fe—FeP_2—BP—FeB—Fe. Alloys with a non-metal content less than 10 atom % were not studied.

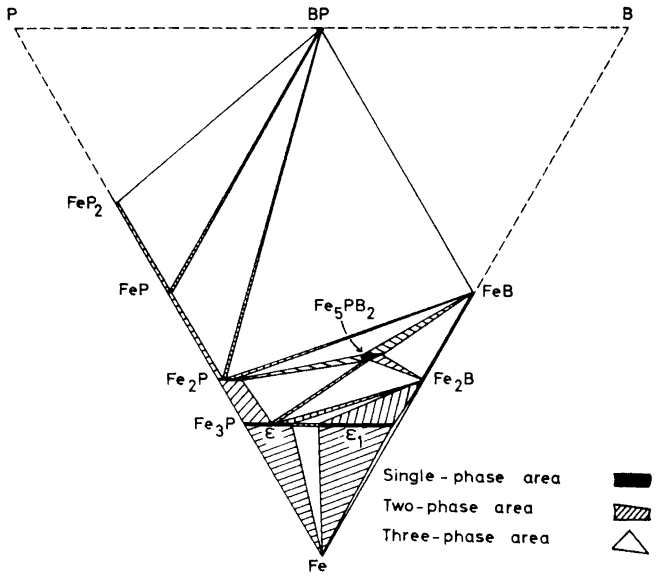

Fig. 1. Isothermal section at 1 000°C of the Fe—P—B system. (Some of the areas are enlarged for clarity).

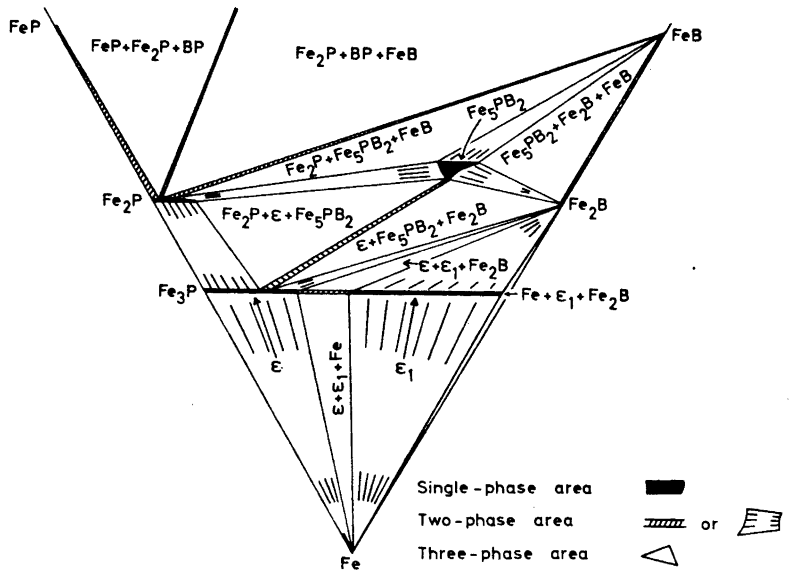

Fig. 2. Isothermal section at 1 000°C of the Fe—P—B system. (Some of the areas are enlarged for clarity. The two-phase area Fe + Fe_2B is not indicated).

The data obtained for the pure binary phases were in agreement with earlier investigations. Phase transformations were not detected in binary and ternary alloys quenched from different temperatures up to the melting point or, for high-melting alloys, up to 1 100°C.

No unit cell variations were found for Fe_2B, FeB and BP in different parts of the system. In ternary alloys, the unit cell of α-iron appeared to be slightly

Table 2. Unit cell dimensions (Å) of Fe_2P, Fe_5PB_2, ε and ε_1 in the various three-phase equilibria. Measurements are made on alloys annealed at 1 000°C for 7—14 days and quenched. The unit cell dimensions of FeP_2, FeP, FeB, Fe_2B and BP are not significantly different from the values quoted in Table 1.

Three-phase equilibrium	Fe_2P		Fe_5PB_2		ε		ε_1	
	a	*c*	*a*	*c*	*a*	*c*	*a*	*c*
FeP + Fe_2P + BP	5.872	3.442						
Fe_2P + BP + FeB	5.872	3.442						
Fe_2P + Fe_5PB_2 + FeB	5.900	3.404	5.493	10.370				
Fe_2P + Fe_5PB_2 + ε	5.923	3.350	5.485	10.349	9.025	4.435		
ε + Fe_5PB_2 + Fe_2B			5.483	10.345	9.013	4.428		
Fe_5PB_2 + FeB + Fe_2B			5.473	10.316				
ε + ε_1 + Fe_2B					8.968	4.414	8.888	4.401
ε + ε_1 + α-Fe					8.968	4.414	8.888	4.401

Table 3. X-Ray and chemical analytical data for $Fe_3P_{1-x}B_x$ alloys.

Alloy	Chemical analysis(weight %)				Phases observed in powder photographs	Calculated composition of ε and ε_1	Lattice parameter		Unit cell volume (Å^3)
	Fe	P	B	Σ			a(Å)	c(Å)	
$Fe_{2.990}P$	84.37	15.65	—	100.02	ε	Fe_3P	ε : 9.107	4.460	369.9
$Fe_{3.092}P$	84.74	15.20	—	99.94	ε + α-Fe	Fe_3P	ε : 9.107	4.460	369.9
$Fe_{3.19}P_{0.92}B_{0.08}$	84.90	13.52	0.43	98.85	ε + α-Fe	$Fe_3P_{0.92}B_{0.08}$	ε : 9.068	4.447	365.7
$Fe_{3.03}P_{0.81}B_{0.19}$	85.88	12.72	1.04	99.54	ε	$Fe_3P_{0.81}B_{0.19}$	ε : 9.022	4.431	360.7
$Fe_{3.17}P_{0.71}B_{0.29}$	87.07	10.85	1.54	99.46	ε + α-Fe	$Fe_3P_{0.71}B_{0.29}$	ε : 8.975	4.415	355.6
$Fe_3P_{0.6}B_{0.4}$	—	—	—	—	ε + ε_1	—	ε : 8.968 ε_1: 8.888	4.414 4.401	355.0 347.7
$Fe_{3.10}P_{0.45}B_{0.55}$	88.78	7.21	3.03	99.02	ε_1 + α-Fe	$Fe_3P_{0.45}B_{0.55}$	ε_1: 8.848	4.387	343.4
$Fe_{3.01}P_{0.35}B_{0.65}$	89.92	5.84	3.75	99.51	ε_1	$Fe_3P_{0.35}B_{0.65}$	ε_1: 8.801	4 370	338 5
$Fe_{3.06}P_{0.24}B_{0.76}$	91.19	4.04	4.37	99.60	ε_1	$Fe_3P_{0.24}B_{0.76}$	ε_1: 8.752	4.353	333.4
$Fe_{2.93}P_{0.16}B_{0.84}$	90.67	2.68	5.06	98.41	ε_1 + Fe_2B	$Fe_3P_{0.17}B_{0.83}$	ε_1: 8.707	4.336	328.7
$Fe_{2.85}P_{0.05}B_{0.95}$	92.32	0.89	5.91	99.12	ε_1 + Fe_2B	$Fe_3P_{0.06}B_{0.94}$	ε_1: 8.649	4.316	322.9

smaller than that of pure iron, but the difference was near the limit of experimental error. This observation is, however, in qualitative agreement with the data obtained by Gale [14] for solid solutions of phosphorus in iron. The pure binary phosphides showed no lattice parameter variation, but in ternary alloys, small variations (detected only at temperatures above 1 100°C) were observed for FeP, larger variations for Fe_2P and very large variations for Fe_3P.

The system contains two new ternary phases in addition to the binary phases already reported. One ternary phase has a crystal structure (see below) corresponding to the formula Fe_5PB_2, but small variations in the unit cell dimensions (see Table 2) indicate deviations from the ideal composition. The other ternary phase has a variable composition corresponding to the formula $Fe_3P_{1-x}B_x$. This phase has a striking structural similarity to Fe_3P (see below). In his investigation of the Fe—P system, Hägg [15] has denoted the Fe_3P phase by the symbol ε. For convenience, this notation is used in the following text for phases with the Fe_3P structure, while the symbol ε_1 is used for phases with the closely similar structure.

Phase-analytical data and unit cell dimensions for a series of alloys with compositions near the line Fe_3P—Fe_3B are collected in Table 3. ε and ε_1 are both tetragonal with similar unit cell dimensions. While the alloys do not contain ε or ε_1 alone, the compositions of these phases can be calculated from the figures in Table 3 assuming:

1) a metal/non-metal atomic ratio equal to 3,
2) a small solid solubility of boron and phosphorus in α-Fe,
3) a small solid solubility of phosphorus in Fe_2B,
4) a negligible effect of the impurities.

The first assumption is supported by the appearance of α-Fe in the alloys with a metal/non-metal atomic ratio larger than 3 and of Fe_2B in the alloys with a ratio smaller than 3. The solubilities of phosphorus and boron in α-Fe are small [4], and judging from the previously mentioned lattice parameter values

for α-Fe in ternary alloys, the simultaneous solubility of the non-metals in α-Fe is also very restricted. Within the limits of experimental error, the lattice parameters of Fe_2B are unchanged in ternary alloys, and this together with crystal-chemical considerations is taken as support of the third assumption. As regards contamination, the main impurities are oxygen and silicon, and the errors in the fourth assumption arise from the extrapolation of results from the quinary system Fe—P—B—O—Si to the ternary system Fe—P—B.

Some information on the influence of impurities was collected from a phase analysis of carefully annealed $Fe_3P_{1-x}B_x$ alloys containing 2—3.5 % oxygen and 0.1—0.2 % silicon. The powder photographs of these alloys contained only lines from the phases in the ternary Fe—P—B system. The absence of diffraction lines belonging to oxygen- or silicon-containing impurity phases may be explained as follows: the impurities are dissolved in the ε, ε_1 or α-Fe lattices, alternatively the impurity phases have a small scattering power, or else they are present in a finely divided state. A microscopic examination revealed the presence in several alloys of small, white globules of boron oxide. This phase was not detected in the powder photographs owing to its small scattering power. However, in the boron-poor alloys at least, boron oxide cannot be the only oxygen-containing phase. As an example, data are quoted for an alloy with the following analysis: iron 86.8 %, phosphorus 8.68 %, boron 0.94 %, silicon $\sim$ 0.2 % and oxygen (by difference) 3.4 %. The powder photograph of this alloy contained lines from α-Fe and ε. The lattice parameters of ε (a = 9.023 Å; c = 4.432 Å) indicate that part of the boron is dissolved in this phase. Even if all the boron were combined with oxygen as B_2O_3, 1.3 % oxygen remains to be accounted for. The possibility of solid solubility of oxygen in ε hardly seems probable. In ternary Fe—P—O alloys, no lattice parameter variations for Fe_3P were observed. The remaining oxygen may therefore be present as an iron oxide or an iron phosphate.

A substantial expansion of the Fe_3P unit cell observed in Fe—P—Si alloys indicates that silicon can substitute for phosphorus in the ε phase. However, if silicon is dissolved in ε or ε_1, the limited amount (0.1—0.2 %) has no serious effect on the lattice parameter determinations.

From the above mentioned observations it is evident that the compositions of ε and ε_1 cannot be corrected for impurities in a simple and accurate way. The compositions of ε and ε_1 given in Table 3 are calculated by disregarding the impurities. A comparison of the data in Table 3 with those obtained for

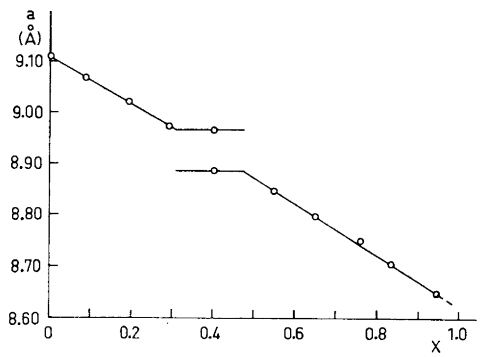

Fig. 3. Variation of the a axis with the boron content in $Fe_3P_{1-x}B_x$.

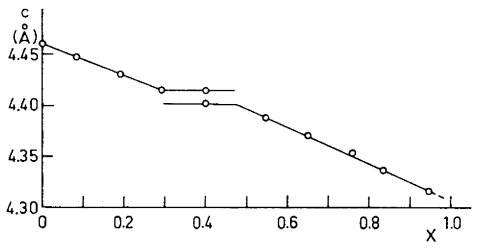

Fig. 4. Variation of the c axis with the boron content in $Fe_3P_{1-x}B_x$.

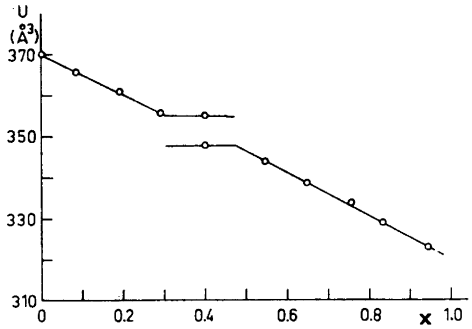

Fig. 5. Variation of the cell volume with the boron content in $Fe_3P_{1-x}B_x$.

the oxygen-rich alloys indicated that the boron/phosphorus atomic ratio in the impurity phases is larger than 1, except possibly in the most phosphorus-rich alloys. This means that the boron/phosphorus ratios for ε and ε_1 given in Table 3, are slightly too high.

In Figs. 3, 4, and 5 curves of lattice parameter *versus* composition are plotted for ε and ε_1. It is seen that at 1 000°C, the boron-rich limit of ε lies close to the composition $Fe_3P_{0.70}B_{0.30}$ and the phosphorus-rich limit of ε_1 close to $Fe_3P_{0.52}B_{0.48}$. The boron-rich limit of ε_1 could not be located with certainty. Since ε_1 does not exist in the binary Fe—B system, a three-phase region α-Fe + ε_1 + Fe_2B should exist in the ternary system. In spite of numerous attempts it was not possible to prepare an alloy containing the three phases in equilibrium. One alloy contained α-Fe and ε_1 for which $a = 8.618$ Å. This value is close to the limiting a-value found by extrapolation of the curve in Fig. 3 to the composition Fe_3B. Unfortunately, the amount of this alloy was too small for accurate chemical analysis. However, it seems highly probable that ε_1 is stable down to a phosphorus/boron atomic ratio less than 0.01. The virtual impossibility of obtaining a three-phase α-Fe + ε_1 + Fe_2B alloy may be attributable both to unfavourable reaction kinetic factors and to the difficulty of detecting very small amounts of a phase by the X-ray technique.

The unit cell variation of Fe_2P in the ternary alloys occurs mainly through phosphorus/boron substitution, but no accurate determination of the single-phase boundaries was attempted. The data indicate a maximum phosphorus/boron substitution of the order of 10 % at 1 000°C. The single-phase area is larger at higher temperatures. The single-phase boundaries of Fe_5PB_2 were not studied in detail. Phase-analytical data for two alloys, one lying in the two-phase region ε + Fe_5PB_2 and the other in the single-phase area close to the region ε + Fe_5PB_2, are given in Table 4. A metal/non-metal atomic ratio larger than 5/3 is indicated. It is felt that small amounts of ε may be present in the apparently single-phase Fe_5PB_2 alloy without being detected in the powder photographs, and that the metal/non-metal atomic ratio may accordingly be smaller than 5.12/3. The boron/phosphorus atomic ratio is, however, definitely larger than 2/1, even assuming the total impurity content to be boron oxide. Small amounts of ε in the alloys would not invalidate this conclusion, since the boron/phosphorous atomic ratio is much smaller in ε than in

Table 4. X-Ray and chemical analytical data for Fe_5PB_2 alloys.

Alloy	Chemical analysis (weight %)				Phases observed in powder photographs	Lattice parameters of Fe_5PB_2	
	Fe	P	B	Σ		a (Å)	c (Å)
$Fe_{5.23}P_{0.95}B_{2.05}$	84.19	8.52	6.38	99.09	$\varepsilon + Fe_5PB_2$	5.485	10.346
$Fe_{5.12}P_{0.92}B_{2.08}$	84.38	8.46	6.63	99.47	Fe_5PB_2	5.485	10.349

Fe_5PB_2. A boron/phosphorus atomic ratio larger than 2/1 is also in accordance with crystal-chemical considerations to be discussed later in this paper.

Some data for the systems Cr—P—B, Mn—P—B, Co—P—B and Ni—P—B

The results from the Fe—P—B system aroused interest in ternary systems containing the transition metal neighbours of iron in the periodic system. Owing to the experimental difficulties, only a very limited number of alloys in selected parts of the systems were investigated.

The Cr—P—B system. To prepare ternary Cr—P—B alloys, temperatures above 1 100°C were found to be necessary, and consequently only limited results were obtained by the silica tube technique. It was found, however, that Cr_3P dissolves boron, as is demonstrated by the measured lattice parameters. For Cr_3P, $a = 9.185$ Å; $c = 4.560$ Å (somewhat different from the values given by Nowotny and Henglein [16], and by Schönberg [17], but in good agreement with those obtained by Lundström [18]), whereas for the ε phase in an alloy with the nominal composition $Cr_3P_{0.8}B_{0.2}$, $a = 9.134$ Å; $c = 4.545$ Å.

The Mn—P—B system. As with Cr_3P and Fe_3P, Mn_3P was also found to dissolve boron. The measured lattice parameters of binary Mn_3P are $a = 9.181$ Å; $c = 4.568$ Å (the c axis differs from the value given by Årstad and Nowotny [19]) whereas for the ε phase in an alloy, quenched from 950°C with the nominal composition $Mn_3P_{0.5}B_{0.5}$ and containing small amounts of Mn_4B, the parameter values are $a = 9.121$ Å; $c = 4.530$ Å. There were no indications that an ε_1 type phase occurs in this system. A ternary phase close to the composition Mn_5PB_2 was found to be isomorphous with Fe_5PB_2. The measured lattice parameters display a similar variation to those of Fe_5PB_2, and are approximately $a = 5.54$ Å; $c = 10.49$ Å.

The Co—P—B system. A phosphide Co_3P of the ε type does not occur in the binary Co—P system [4]. Nevertheless, ternary phases of both the ε and ε_1 types exist in the ternary Co—P—B system. The lattice parameters of ε, measured in alloys quenched from 950°C, ranged from $a = 8.780$ Å; $c = 4.336$ Å (phosphorus-rich) to $a = 8.752$ Å; $c = 4.326$ Å (boron-rich). The corresponding values for the ε_1 phase were $a = 8.686$ Å; $c = 4.303$ Å; and $a = 8.673$; $c = 4.297$ Å. These values suggest that the homogeneity ranges are much smaller than those for the corresponding iron phases. Although compositions were not determined accurately, compositions close to $Co_3P_{0.5}B_{0.5}$ for the ε

phase and to $Co_3P_{0.3}B_{0.7}$ for the ε_1 phase were indicated. Lattice parameter variations of Co_2P and CoP in ternary alloys indicated some boron solubility in these phases. The Co—P—B system also contains a ternary phase of the Fe_5PB_2 type, with small lattice parameter variations. The approximate unit cell dimensions for Co_5PB_2 were found to be $a = 5.42$ Å; $c = 10.20$ Å.

The Ni—P—B system. In contrast to the above-mentioned systems, Ni_3P does not dissolve any appreciable amounts of boron. Within the limits of experimental error the unit cell dimensions of Ni_3P were unchanged in ternary Ni—P—B alloys. The rather complicated Ni—P—B system was not studied in any detail. Changes of the Ni_2P unit cell dimensions were observed which indicated a substantial boron solubility in this phase.

II. THE CRYSTAL STRUCTURES OF Fe_3P, $Fe_3P_{0.37}B_{0.63}$ AND Fe_5PB_2

Among the phases occurring in the ternary Fe—P—B system, the crystal structure types have been determined [10-12,20-25] for Fe_2B, FeB, Fe_3P, Fe_2P, FeP, FeP_2 and BP (see Table 1). Accurate interatomic distances have at present been determined only for Fe_2P and BP.

The subsequent part of this paper contains accounts of the structure determinations of the ε_1 and Fe_5PB_2 phases, and of the refinement of the Fe_3P structure.

Experimental

Single crystal fragments were selected from alloys prepared as described above. Fragments with uniform cross-sections not larger than 0.05 mm were chosen so that absorption effects should be as low as possible.

Unit cell dimensions were determined using Guinier-type powder cameras with Cr$K\alpha$ radiation, giving an estimated accuracy of 0.04 %.

Weissenberg photographs were taken using MoK radiation and the multiple-film technique with thin iron foils between successive films. The intensities were estimated visually. No direct corrections for absorption were made. Corrections for Lorentz and polarisation factors together with Fourier summations, structure factor calculations, and calculations of interatomic distances were made on the electronic digital computer BESK using programmes devised by Westman *et al.*[26], Åsbrink *et al.*[27] and Liminga [28]. Atomic scattering factors were taken from tables given by Thomas and Umeda [29] for iron, by Tomiie and Stam [30] for phosphorus and by Ibers [31] for boron. The real part of the dispersion correction, taken from the table by Dauben and Templeton [32], was included in the structure factor calculations. Standard deviations of the atomic parameters were estimated by Cruickshank's [33] formula. (Lists of observed and calculated structure factors can be obtained from this Institute on request.)

The structure of Fe_3P

Fe_3P is isostructural with Ni_3P, the structure of which was determined by Aronsson [22]. The space group of Ni_3P is $I\,\bar{4}$, with 24 nickel atoms in three sets of eightfold positions and 8 phosphorus atoms in one eightfold position.

The Weissenberg photographs of Fe_3P were taken about the a-axis and the c-axis. The intensity data were consistent with the proposed structure, and the atomic positions were refined starting with the parameter values given by Aronsson for Ni_3P. Successive difference syntheses were made in the ab and ac projections. 138 $F(hk0)$- and 83 $F(h0l)$-values were measured, and after

the final refinements R-values of 0.058 were obtained for both $F(hk0)$ and $F(h0l)$. (The very strong (004) reflexion was omitted because of serious extinction effects.)

Isotropic temperature factors with $B = 0.37_8$ Å^2 for $F(hk0)$ and $B = 0.41_4$ Å^2 for $F(h0l)$ were applied. The differences between the two sets of x and y parameters obtained from the ab and ac projections were smaller than the standard deviations.

The final structural data for Fe_3P are as follows,

Space-group $I\ \bar{4}\ -(S_4^2)$ $a = 9.107$ Å; $c = 4.460$ Å; $U = 369.9$ Å^3; $Z = 8$.

Atoms in 8(g)	x	$\sigma(x)$	y	$\sigma(y)$	z	$\sigma(z)$
Fe_I	0.0793	0.0002	0.1059	0.0002	0.2338	0.0008
Fe_{II}	0.3605	0.0002	0.0310	0.0002	0.9860	0.0008
Fe_{III}	0.1717	0.0002	0.2195	0.0002	0.7548	0.0008
P	0.2921	0.0004	0.0454	0.0004	0.4903	0.0014

Interatomic distances are given in Table 5. A projection of the structure on the basal plane is given in Fig. 6.

The structure of ε_1 with the composition $Fe_3P_{0.37}B_{0.63}$

The powder photographs of the ε_1 phase show strong similarities to those of the ε phase. The diffraction lines can be indexed on the basis of tetragonal unit cells with dimensions similar to those of ε. Reflexions with $h + k + l = 2n + 1$ are present, however, showing that the cell is primitive.

A single crystal of ε_1 suitable for X-ray work was found in an alloy with the nominal composition $Fe_3P_{0.35}B_{0.65}$. The powder photographs of this alloy (powder data are listed in Table 6) gave the following lattice parameter values for ε_1: $a = 8.812$ Å, $c = 4.375$ Å. From Figs. 3 and 4 it is seen that the real composition of the ε_1 sample is close to $Fe_3P_{0.37}B_{0.63}$.

The Weissenberg photographs indicated the Laue symmetry $4/m$. The following extinctions were observed: $(hk0)$ for $h + k = 2n + 1$, and $(00l)$ for $l = 2n + 1$. This points to the space group $P\ 4_2/n$. The $F(hk0)$ values for ε_1

Table 5. Interatomic distances in Fe_3P (Å). Distances shorter than 3.6 Å listed.

	Fe_I	Fe_{II}	Fe_{III}	P
Fe_I	2.41_0, 2.69_3 (2), 2.92_3 (2)	2.71_0, 2.87_1 3.53_6	2.51_8, 2.67_9, 2.77_1, 2.78_7, 2.83_3	2.31_7, 2.38_3, 3.55_5
Fe_{II}	2.71_0, 2.87_1, 3.53_6	2.60_3, 2.79_6 (2), 2.98_9 (2)	2.52_8, 2.58_6, 2.63_9, 3.52_0	2.30_1, 2.33_3, 2.33_8, 2.34_1
Fe_{III}	2.51_8, 2.67_9, 2.77_1, 2.78_7, 2.83_3	2.52_8, 2.58_6, 2.63_9, 3.52_0	2.70_5 (2)	2.26_0, 2.35_4, 2.40_7, 3.59_0
P	2.31_7, 2.38_3, 3.55_5	2.30_1, 2.33_3, 2.33_8, 2.34_1	2.26_0, 2.35_4, 2.40_7, 3.59_0	3.47_2 (2), 3.58_8 (2)

Table 6. Powder data for ε_1 with the composition $Fe_3P_{0.37}B_{0.63}$. (Cr$K\alpha$ radiation, $\lambda = 2.2909$ Å).

hkl	$\sin^2\Theta_{obs} \times 10^4$	$\sin^2\Theta_{calc} \times 10^4$	$p\,F^2_{calc} \times 10^{-3}$	I_{obs}
100	337	338	0.4	v.v.w
200	—	676	0.0	—
101	—	854	0.0	—
111	—	1 023	1.1	—
220	1 352	1 352	10.6	v.w
201	1 362	1 361	20.4	w
211	1 531	1 530	0.0	v.w
121			4.0	
310	1 691	1 690	7.9	v.w
130			0.8	
221	2 036	2 037	9.0	v.w
301	2 206	2 206	36.8	w
311	2 374	2 375	18.1	m+
131			136.2	
400	2 702	2 703	20.9	w
002	2 740	2 741	23.2	w
321	2 881	2 882	349.4	st+
231			176.4	
330	3 043	3 041	155.6	m
112	3 079	3 079	327.4	st
420	3 377	3 379	231.2	m+
240			0.1	
401	3 387	3 389	90.1	m—
202	3 418	3 418	89.5	m—
411	3 556	3 557	75.7	st+
141			365.7	
212	3 588	3 587	0.5	v.w
122			9.9	
331	3 726	3 726	36.9	w
421	4 063	4 064	10.1	m—
241			57.9	
222	4 093	4 093	132.7	m
302	4 264	4 262	16.9	w
510	4 393	4 393	4.3	m
150			148.8	
312	4 431	4 431	210.0	st—
132			0.0	
431	4 910	4 909	14.4	w
341			1.7	
501			4.3	
322	—	4 939	0.0	—
232			0.8	

are remarkably similar to the corresponding values for Fe_3P, and it was concluded that the two structures must look almost identical when viewed in projection on the basal plane. From this argument, and from a consideration of the different symmetry elements operating in the two space groups $I\bar{4}$ and $P4_2/n$, the following model was proposed for the structure of ε_1. The atomic

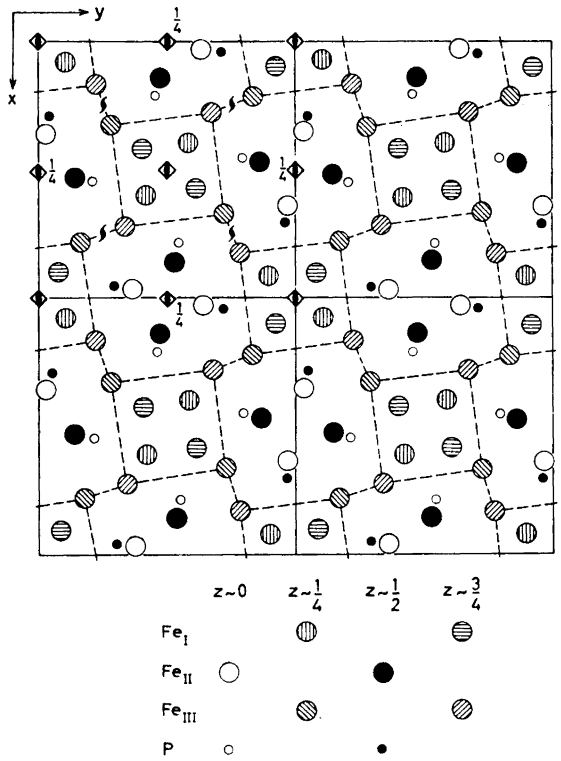

Fig. 6. The structure of Fe_3P projected on the basal plane.

coordinates for the asymmetric part of the Fe_3P structure (referring to the origin at $\bar{4}$ in $I\,\bar{4}$) are related to the corresponding coordinates in ε_1 (referring to $\bar{1}$ as the origin in $P\,4_2/n$) as follows:

$I\,\bar{4}$: atom in $x,\ y,\ z$
$P\,4_2/n$: corresponding atom in $x + \frac{3}{4},\ y + \frac{1}{4},\ z$

The electron density projections $\varrho(xy)$ and $\varrho(xz)$ were calculated for ε_1 on this basis. The signs of the structure factors were taken from the iron contributions only. In addition to the expected iron maxima, other maxima corresponding to an $8(h)$ position were discernible. The heights of these maxima were seen to correspond roughly to 9/26 of the iron maxima. Since no indications of superstructure reflexions could be detected, it was concluded that the boron and phosphorus atoms occupy one $8(h)$ position randomly.

The ε_1 structure was refined by the same methods as those described for Fe_3P. A weighted average of the atomic scattering factors for boron and phosphorus was used in the structure factor calculations. After the final refinements the following R-values were obtained: 59 observed $F(hk0)$ values $R = 0.104$, 41 observed $F(h0l)$ values $R = 0.108$. (The very strong (004) reflexion was

omitted because of extinction effects). Over all temperature factors with $B = 0.70$ Å^2 for $F(hk0)$ and $B = 0.65$ Å^2 for $F(h0l)$ were applied. The corresponding x and y parameters obtained from the ab and ac projections agreed within the limits of the standard deviations.

The satisfactory agreement between observed and calculated structure factors shows that the initial assumptions made for the ε_1 structure are most probably correct.

Structure data obtained for ε_1 with the composition $Fe_3P_{0.37}B_{0.63}$ are as follows:

Space group $P\ 4_2/n$ — (C_{4h}^4) $a = 8.812$ Å; $c = 4.375$ Å; $U = 339.7$ Å^3. (Origin at $\bar{1}$).

Atoms in 8(g)	x	$\sigma(x)$	y	$\sigma(y)$	z	$\sigma(z)$
Fe_I	0.1678	0.0004	0.6422	0.0004	0.731_2	0.0017
Fe_{II}	0.1115	0.0004	0.2813	0.0004	0.518_7	0.0017
Fe_{III}	0.0742	0.0004	0.5317	0.0004	0.242_4	0.0017
(0.37P + 0.63B) randomly	0.045_0	0.0013	0.294_9	0.0013	0.016	0.006

Interatomic distances are listed in Table 7. A projection of the structure on the basal plane is shown in Fig. 7.

Discussion of the ε (Fe_3P) and ε_1 structures

The packing of the atoms in ε and ε_1 is somewhat complicated. In order to illustrate the difference between the two structures more clearly, the following simple description may be convenient.

The Fe_I atoms are arranged in slightly distorted tetrahedra near the $\bar{4}$ axes with inversion at $z = 0$ in ε, and near the 4_2 axes in ε_1. The Fe_I tetrahedra are situated within larger (distorted) tetrahedra of Fe_{III} atoms. The Fe_I and Fe_{III} tetrahedra form a network throughout the structure (indicated in Figs. 6 and 7) leaving large "channels" along the $\bar{4}$ axes with inversion at $z = \frac{1}{4}$. In these "channels", (distorted) tetrahedra of Fe_{II} atoms are situated within

Table 7. Interatomic distances in $Fe_3P_{0.37}B_{0.63}$ (Å). Distances shorter than 3.5 Å listed. (X = non-metal atoms).

	Fe_I	Fe_{II}	Fe_{III}	X
Fe_I	2.39, 2.76 (4)	2.68, 2.78, 3.35	2.49, 2.57, 2.63, 2.72, 2.77	2.25, 2.27, 3.48
Fe_{II}	2.68, 2.78, 3.35	2.50, 2.69 (2) 2.94 (2)	2.50, 2.54, 2.55, 3.36	2.23, 2.24 2.26, 2.28
Fe_{III}	2.49, 2.57, 2.63 2.72, 2.77	2.50, 2.54, 2.55, 3.36	2.55, 2.67	2.17, 2.31 2.32, 3.47
X	2.25, 2.27 3.48	2.23, 2.24 2.26, 2.28	2.17, 2.31 2.32, 3.47	3.32 (2) 3.50 (2)

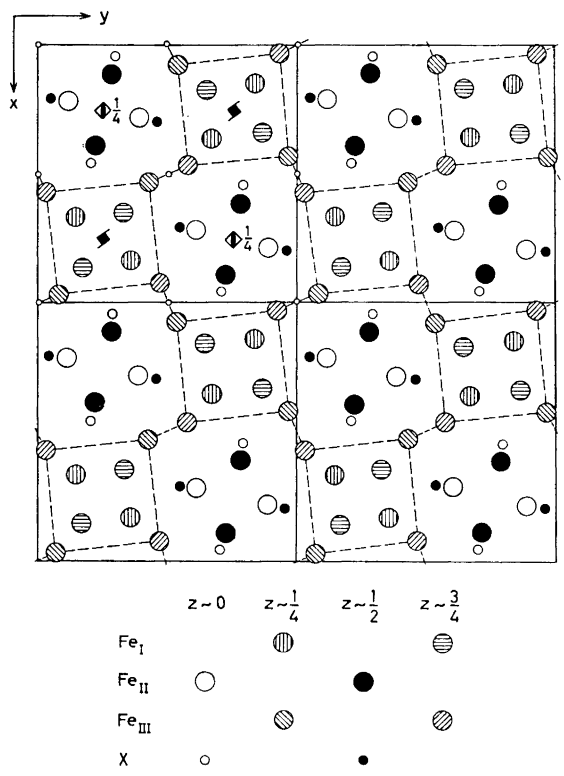

Fig. 7. The structure of ε_1 projected on the basal plane.

larger (distorted) tetrahedra of non-metal atoms. Whereas the network of Fe_I and Fe_{III} tetrahedra is almost identical in the two structures, the arrangement of the Fe_{II} and non-metal tetrahedra is different. In the ε structure the Fe_{II} and non-metal tetrahedra in one "channel" are translated a distance equal to $c/2$ along the tetragonal axis with respect to the tetrahedra with equal orientation in the four adjacent "channels". In the ε_1 structure the Fe_{II} and non-metal tetrahedra at the same c-level have approximately the same orientation in all "channels".

The above description shows that the main difference between the two structures lies in the "long-range" configuration of the atoms. The near environment of corresponding atoms in ε and ε_1 is very similar. One special feature is worth mentioning. There is one very short Fe_I—Fe_I distance in both ε and ε_1. The two Fe_I atoms have six close iron neighbours in common, and the short distance can be explained from geometric considerations as was shown by Frank and Kasper [34]. The Fe_I—Fe_I distance in ε_1 (2.39 Å) is only slightly shorter than that in ε (2.41 Å). In general, however, the Fe—Fe as well as the Fe—X (X = non-metal) distances are 0.07—0.08 Å shorter in ε_1 than in ε, as is shown by the values listed in Table 8.

Table 8. Average Fe—Fe and Fe—X (X = non-metal) distances in ε and ε_1.

Neighbours	Average in Fe_3P (Å)	Average in $Fe_3P_{0.37}B_{0.63}$ (Å)	Difference (Å)
Fe_I — 12Fe	2.73_4	2.67_4	$+ 0.06_0$
Fe_I — 2X	2.35_0	2.25_7	$+ 0.09_3$
Fe_{II} — 10Fe	2.75_1	2.68_0	$+ 0.07_1$
Fe_{II} — 4X	2.32_8	2.25_3	$+ 0.07_5$
Fe_{III} — 10Fe	2.67_5	2.59_8	$+ 0.07_7$
Fe_{III} — 3X	2.34_0	2.27_0	$+ 0.07_0$
X — 9Fe	2.33_7	2.26_0	$+ 0.07_7$

It might be expected, that the morphotropic transition from ε to ε_1 is dependent upon the size-effect of the non-metal atoms. However, from the comments made above, it appears that the near environment of the atoms found in ε_1 could be attained equally well in a structure of the ε type merely by a contraction of the unit cell and small adjustments of the atomic parameters. An explanation of the transition in terms of the size effect is therefore not obvious. Judging from the close similarity between ε and ε_1, the differences in free energy between the two structures must certainly be very small.

The crystal structure of Fe_5PB_2

Excellent single crystals of Fe_5PB_2 were often found in the annealed alloys. They occurred mostly as square plates with the *c* axis perpendicular to the plane and the *a* axes along the diagonals of the square.

Table 9. Powder data for an alloy containing Fe_5PB_2. (Cr*Ka* radiation, $\lambda = 2.2909$ Å).

hkl	$\sin^2\Theta_{obs} \times 10^4$	$\sin^2\Theta_{calc} \times 10^4$	$p\,F^2_{calc} \times 10^{-3}$	I_{obs}
002	—	492	0.0	—
110	872	873	6.0	v.w
112	1 365	1 365	16.3	w
200	1 747	1 746	8.9	v.w
004	1 967	1 966	47.3	w+
202	2 237	2 238	37.4	w+
211	2 306	2 306	278.3	st—
114	2 840	2 840	220.4	m+
—	3 241	—	—	v.w*
213	3 290	3 289	644.1	st +
220	3 493	3 492	136.7	m
204	3 712	3 713	473.0	st
222	—	3 984	3.4	—
310	4 365	4 366	463.6	st
006	4 424	4 424	74.7	w+
312	—	4 858	4.5	—

* The (211) reflexion from Fe_2B.

A single crystal was selected from an alloy, containing Fe_5PB_2 (lattice parameters, $a = 5.482$ Å; $c = 10.332$ Å) together with traces of Fe_2B. The powder data for this alloy are given in Table 9.

The Weissenberg photographs showed that the Laue symmetry is $4/mmm$, and the possible space groups I $4/mcm$, $I\,\bar{4}c2$ and $I\,4cm$ were indicated. From the unit cell dimensions and the general distribution of the intensities it seemed highly probable that Fe_5PB_2 should be isostructural with Cr_5B_3, the structure of which has been determined by Bertaut and Blum [35].

Starting with this assumption the electron density projection $\varrho(xz)$ was evaluated for Fe_5PB_2. The electron density map indicated ordered positions for the boron and phosphorus atoms, in a similar fashion to that found by Aronsson [36] for the boron and silicon atoms in Mo_5SiB_2.

The atomic parameters in Fe_5PB_2 were refined in the usual way. Large discrepancies between F_c and F_o values for the strongest reflexions (especially (004), (006), (008), (204), (400) and (600)) were, however, observed. Another set of intensity data were obtained using a very small crystal with a different habit to that of the first. Although the discrepancies for the strongest reflexions were reduced, they remained noticeable. Since both crystals were so small that the absorption effects could not be very serious, the discrepancies were thought to arise largely through extinction. This is consistent with the extremely perfect external shape of the crystals. In the subsequent refinement, the contributions from the above-mentioned reflexions were neglected. The final R-value for the 64 observed $F(h0l)$-values was 0.13 for the smallest crystal and 0.18 for the larger crystal. With the omission of the six strongest reflexions, the R-value was 0.08 for both crystals. An isotropic temperature factor with $B = 0.20$ Å^2 was applied.

The following structure data were obtained for Fe_5PB_2:

Space-group $I\,4/mcm$ — (D_{4h}^{18}) $a = 5.482$ Å; $c = 10.332$ Å; $U = 310.5$ Å^3; $Z = 4$.

			x	$\sigma(x)$	z	$\sigma(z)$
16	Fe_I	in 16(l)	0.1690	0.0005	0.1400	0.0003
4	Fe_{II}	in 4(c)				
8	B	in 8(h)	0.375	—		
4	P	in 4(a)				

Interatomic distances are listed in Table 10.

On account of the marked extinction effects in the intensity material, no attempt was made to refine the scattering parameters for the different atomic positions. The difference between the scattering parameters of the 8(h) and the 4(a) atoms was so large, however, that the conclusion regarding the ordered distribution of boron and phosphorus atoms must be essentially correct.

Discussion of the Fe_5PB_2 structure

The Cr_5B_3 ($D\,8_l$) type of structure has been thoroughly described and discussed by Parthé *et al.*[37] and by Aronsson [36], among others. Several silicoborides crystallize with this structure. Data given by Aronsson [36,2] show that lattice parameter variations for Mo_5SiB_2 and Fe_5SiB_2 are very similar to those for Fe_5PB_2. The smallest unit cell volume is found in boron-rich alloys,

Table 10. Interatomic distances in Fe_5PB_2 (Å). Distances shorter than 3.0 Å listed.

	Fe_I	Fe_{II}	B	P
Fe_I	2.60, 2.62, 2.88 (4) 2.89, 2.93 (2)	2.50 (2)	2.18, 2.16	2.33 (2)
Fe_{II}	2.50 (8)	—	2.17 (4)	2.58 (2)
B	2.18 (4) 2.16 (2)	2.17 (2)	1.94	—
P	2.33 (8)	2.58 (2)	—	—

which may indicate that boron substitutes for silicon and phosphorus to some extent. This is in accordance with the phase-analytical data quoted above. It must be pointed out, however, that the lattice parameter variations may also depend on simultaneous variations of the metal/non-metal ratio.

Aronsson [36] mentions that there are two types of "hole" in the metal atom lattice of the Cr_5B_3 type, which permit non-metal atoms of two different sizes to be neatly accomodated in the structure. The smaller non-metal atoms are situated in trigonal prismatic holes and the larger non-metal atoms in anti-prismatic holes. If in Mo_5SiB_2, the molybdenum radius is 1.38 Å the "hole" radii are 0.98 Å for the trigonal prismatic and 1.18 Å for the anti-prismatic holes. The corresponding values in Fe_5PB_2 (iron radius 1.26 Å) are 0.93 Å and 1.08 Å. It is seen that the sizes of the holes correspond roughly to the normal tetrahedral radii $r_B = 0.88$ Å; $r_P = 1.10$ Å and $r_{Si} = 1.17$ Å. The size-factor considerations indicate that boron may substitute for silicon and phosphorus, whereas substitution for boron by the larger non-metals is less probable.

General remarks on Me—P—B systems

The metal-rich transition metal borides, silicides and phosphides are known to have many crystal-chemical properties in common, and the present investigation gives further support to this general picture. In this respect the phosphorus/boron substitution in binary phosphide structures is especially noteworthy. Furthermore, the similarities between corresponding Me—P—B and Me—Si—B systems are very marked. Accordingly, a crystal-chemical discussion of transition metal phosphides and their relations to silicides and borides seems warranted, but is deferred to a later paper.

Acknowledgements. This work has been financially supported by the *Swedish State Council of Technical Research* and by the *Air Force Office of Scientific Research of the Air Research and Development Command, United States Air Force,* through its European Office under Contract No. AF 61(052)—40. Facilities for use of the electronic digital computer BESK were given by the *Swedish Board For Computing Machinery.*

The author wishes to thank Prof. G. Hägg for his encouraging interest and valuable comments on the manuscript. The author is indebted to Dr. B. Aronsson for valuable hints and many stimulating discussions during the investigation. Thanks are also due to Dr. L. Gustafsson for her very careful approach to the problems of chemical analysis.

REFERENCES

1. Aronsson, B. and Lundgren, G. *Acta Chem. Scand.* **13** (1959) 433.
2. Aronsson, B. and Engström, I. *Ibid.* **14** (1960) 1403.
3. Nydahl, F. *Lantbrukshögsk. Ann.* **10** (1942) 114.
4. Hansen, M. *Constitution of binary alloys. Mc Graw-Hill, New York-Toronto-London* 1958.
5. Heimbrecht, M. and Biltz, W. *Z. anorg. Chem.* **242** (1939) 233.
6. Fruchart, R. *C.r. Acad. Sci. Paris* **247** (1958) 1464.
7. Besson, M. A. *Ibid.* **113** (1891) 78.
8. Moissan, H. *Ibid.* **113** (1891) 624.
9. Moissan, H. *Ibid.* **113** (1891) 726.
10. Rundqvist, S. *XVI*^{e} *Congr. Int. de Chim. Pure et App., Section de Chim. Min., Sedes Paris* 1957, 539.
11. Popper, P. and Ingles, T. A. *Nature* **179** (1957) 1075.
12. Perri, J. A., La Placa, S. and Post, B. *Acta Cryst.* **11** (1958) 310.
13. Matkovich, V. I. *Ibid.* **14** (1961) 93.
14. Gale, B. *Acta Met.* **7** (1959) 420.
15. Hägg, G. *Nova Acta Regiae Soc. Sci. Upsaliensis,* Ser. IV, **7** (1929) No. 1.
16. Nowotny, H. and Henglein, E. *Z. anorg. Chem.* **239** (1938) 14.
17. Schönberg, N. *Acta Chem. Scand.* **8** (1954) 226.
18. Lundström, T. *Ibid.* **16** (1962). *In press.*
19. Årstad, O. and Nowotny, H. *Z. physik. Chem.* **B 38** (1937) 356.
20. Hägg, G. *Z. physik. Chem.* **B 11** (1930) 152.
21. Bjurström, T. *Arkiv Kemi, Mineral. Geol.* **11 A** (1933) No. 5.
22. Aronsson, B. *Acta Chem. Scand.* **9** (1955) 137.
23. Rundqvist, S. and Jellinek, F. *Ibid.* **13** (1959) 425.
24. Fylking, K.-E. *Arkiv Kemi Mineral Geol.* **11 B** (1935) No. 48.
25. Meisel, K. *Z. anorg. Chem.* **218** (1934) 360.
26. Westman, S., Blomqvist, G. and Åsbrink, S. *Arkiv Kemi* **14** (1959) 535.
27. Åsbrink, S., Blomqvist, G. and Westman, S. *Ibid.* **14** (1959) 545.
28. Liminga, R. Program available at BESK.
29. Thomas, L. H. and Umeda, K. *J. Chem. Phys.* **26** (1957) 293.
30. Tomiie, Y. and Stam, C. H. *Acta Cryst.* **11** (1958) 126.
31. Ibers, J. A. *Ibid.* **10** (1957) 86.
32. Dauben, C. H. and Templeton, D. H. *Ibid.* **8** (1955) 841.
33. Cruickshank, D. W. J. *Ibid.* **2** (1949) 65.
34. Frank, F. C. and Kasper, J. S. *Ibid.* **11** (1958) 184.
35. Bertaut, F. and Blum, P. *C.r. Acad. Sci. Paris* **236** (1953) 1055.
36. Aronsson, B. *Acta Chem. Scand.* **12** (1958) 31.
37. Parthé, E., Lux, B. and Nowotny, H. *Monatsh.* **86** (1955) 859.

Received June 21, 1961.